Possible mechanism of charge transport and dielectric relaxation in $SrO-Bi_2O_3-B_2O_3$ glasses

Koushik Majhi, K. B. R. Varma,[a] and K. J. Rao
Materials Research Centre, Indian Institute of Science, Bangalore 560012, India

(Received 15 July 2009; accepted 16 September 2009; published online 28 October 2009)

Transparent $SrBi_2B_2O_7$ glasses were prepared via melt-quenching technique and characterized using differential scanning calorimetry and x-ray powder diffraction. The ac conductivities of the glasses were studied as a function of frequency (100 Hz–10 MHz) at different temperatures. The frequency dependence of conductivity has been analyzed using Almond–West expression. The exponent n was nearly unaffected by temperature. Impedance and modulus spectroscopies were employed to further examine the electrical data. Dielectric relaxation exhibited a stretched exponential behavior with a stretching exponent β independent of temperature. From conductivity analysis we have proposed that the charge transport occurs through the participation of nonbridging oxygen (NBO), which switches positions in a facile manner. The stretched exponential behavior appears to be a direct consequence of the NBO switching mechanism of charge transport. © *2009 American Institute of Physics*. [doi:10.1063/1.3246810]

I. INTRODUCTION

Transparent glasses grafted with polar/nonlinear optic crystallites have great potential for applications. Among the known borate glasses those containing Bi_2O_3 are of particular interest because of their long infrared cutoff and high third order nonlinear optical susceptibility, which make these glasses ideal candidates for making infrared transmission components, ultrafast optical switches, and photonic devices besides a scope of other applications.[1,2] These glasses also have potential applications as glass ceramics as substrates for optical and electronic devices, thermal and mechanical sensors, and reflecting windows.[3–11] Bismuth borate glasses have been studied intensively in recent decades for their electrical, optical, and thermal properties[12–14] also. Recently considerable attention has been paid to noncentrosymmetric bismuth borate based compounds for their possible applications as piezoelectric, ferroelectric, pyroelectric, and nonlinear optical device materials.[15–18] Various single crystal borates including $LaGeBO_5$, β-BaB_2O_4, BiB_3O_6, and $BaBiBO_4$ have been investigated and reported to possess promising physical properties.[19–22]

We have been making systematic efforts to explore the possibilities of employing bismuth borate based glass system containing nano/micropolar crystals of the same phase for the pyroelectric, electro-optic, and nonlinear device applications.[16–18] Recently $SrBi_2B_2O_7$ (SBBO) single crystal was reported to belong to polar space group $P6_3$.[23] Keeping the potential applications of transparent glass and glass-nano/microcrystal composites in view, attempts were made to fabricate SBBO glasses and glass-nano/microcrystals of SBBO in their own transparent glass matrix[24] and examine their ferroelectric, pyroelectric, and nonlinear optical properties.

In order to understand the behavior of these materials in ac electrical fields keeping in view their device applications, we have performed conductivity studies on as-quenched SBBO glasses over a range of temperatures and frequencies. The results are presented and discussed in this paper.

II. EXPERIMENTAL

SBBO glasses were fabricated via the conventional melt-quenching technique. Required quantities of $SrCO_3$ (99.95%, Aldrich), Bi_2O_3 (99.9%, Merck), and B_2O_3 (99.9%, Aldrich) were mixed and melted in a platinum crucible at 1373 K for 1 h. Melts were quenched by pouring onto a steel bloch and pressing with another steel bloch to obtain 1–1.5 mm thick glass-plates. X-ray powder diffraction (XRD) study was performed at room temperature on the as-quenched samples to confirm their amorphous nature. The differential scanning calorimetry (DSC) (model Diamond DSC, Perkin-Elmer) runs were carried out in the 550–900 K temperature range in dry nitrogen ambience. The as-quenched glass-plates (there were no heterogeneities present before DSC runs) weighing 15 mg were used for the experiments.

Dielectric studies on the as-quenched glass samples were carried out as a function of frequency (100 Hz–10 MHz) and temperature using an impedance/gain phase analyzer (HP 4194A). For this purpose the samples were sputtered with gold, and silver leads were attached using silver epoxy.

III. RESULTS AND DISCUSSION

Figure 1 shows the typical DSC trace recorded for the as-quenched SBBO glass-plate at a heating rate of 10 K/min. An endotherm around 670 K followed by an exotherm at 730 K was observed. They were associated with the glass transition (T_g) and the onset of the crystallization temperature (T_{cr}), respectively, for the as-quenched samples. The x-ray diffraction pattern obtained for the as-quenched SBBO glass-plate is shown in the inset of Fig. 1. This pattern reveals the overall amorphous nature of the as-quenched sample.

[a]Electronic mail: kbrvarma@mrc.iisc.ernet.in.

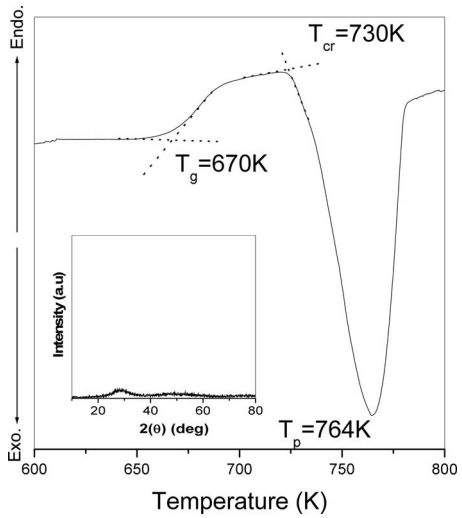

FIG. 1. DSC trace for the as-quenched SBBO glass-plate. Inset shows the XRD pattern for the as-quenched glass.

A. ac conductivity studies

The temperature dependence of the ac conductivity at two different frequencies is shown in Fig. 2. The ac conductivities are nearly temperature independent at low temperatures at both the extreme frequencies (100 Hz and 1 kHz) used in our study. At high temperatures the curves tend to merge with each other and with a constant slope. This frequency independent behavior is attributed to the dominant contribution from the dc conduction at high temperature. The solid line that is shown in Fig. 2 is the linear fit, and the corresponding activation energy is about 1.23 eV.

The frequency dependence of ac conductivity at various temperatures is shown in Fig. 3. It is noticed that in the temperature range from 303 to 503 K, the high frequency conductivities tend to become independent of temperature. At low temperatures the conductivities exhibit a plateau, and the corresponding conductivity values increase (303–503 K)

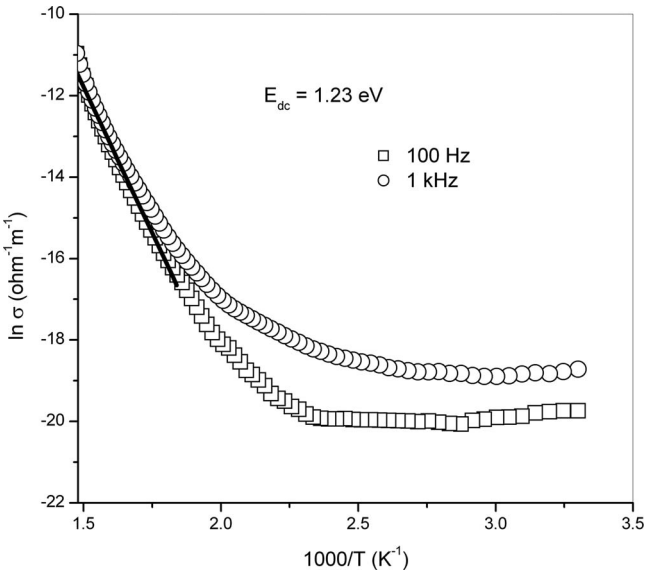

FIG. 2. Temperature dependence of ac conductivity at two different frequencies.

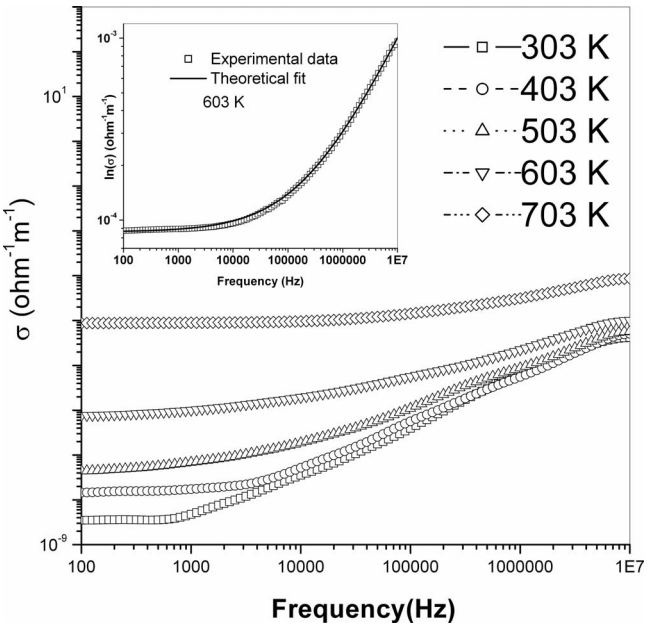

FIG. 3. Variation in ac conductivity as a function of frequency at different temperatures. Inset shows the experimental and theoretical fits for ac conductivity as a function of frequency at 603 K.

with an increase in frequency. Overall behavior in the conductivity elbow regions follows characteristic ω^n dependence. At the highest temperatures (703 K), the flat conductivity plateau spreads over the entire range of frequencies used in our studies. The characteristic ω^n dependence sets in at much higher frequencies and temperatures.

Frequency dispersion of conductivity in solids is generally analyzed using power law of the type[25]

$$\sigma(\omega) = \sigma_{dc} + A\omega^n = \sigma_{dc}\left[1 + \left(\frac{\omega}{\omega_h}\right)^n\right], \quad (1)$$

where σ_{dc} is the (frequency independent) dc conductivity at the particular temperature. A is a temperature dependent constant, n is the power law exponent, which varies from zero to one depending on temperature, and ω_h is the hopping frequency of the charge carrier ion. The exponent n is attributed to the interaction between the charge carrier ion with the frame work carrying the balancing charge. According to many body interaction model,[25] n represents the interaction between all dipoles participating in the polarization process. A unit value of n implies a pure Debye case, where the interaction between any two dipoles is negligible. The characteristic frequency ω_h is obtained from the experimental data by equating $\sigma(\omega_h)=2\sigma_{dc}$ as evident from Eq. (1) (Almond *et al.*[26,27]). The hopping frequency (ω_h) is considered as the appropriate parameter for the scaling of the conductivity spectra for the glasses wherever dielectric loss peak maxima or static dielectric constant value cannot be measured accurately.

The SBBO glass obeys Eq. (1) (the so-called universal power law), and a typical fit of Eq. (1) to the experimental data is shown in the inset of Fig. 3. ac conductivity spectra for different temperatures are fitted to Eq. (1), and the parameters n, σ_{dc}, and ω_h are extracted. The variation in n as a function temperature is depicted in Fig. 4. It is interesting to

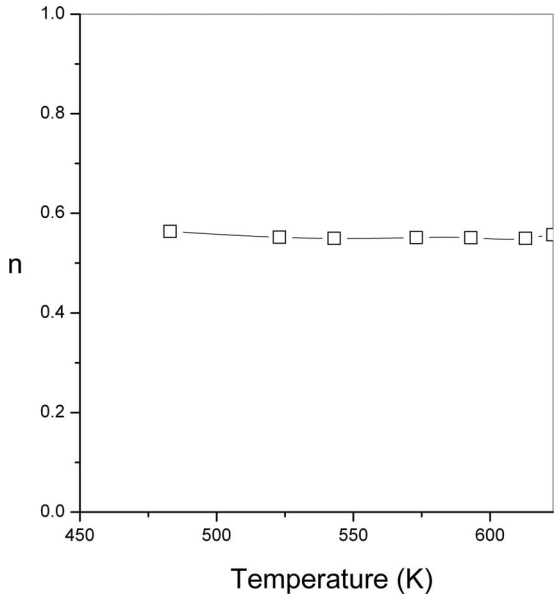

FIG. 4. Variations in the critical exponent n with temperature (lines are drawn as a guide for the eye).

note that the values of n are almost constant. Such a behavior of n is already known in borate glasses.[28] Another general characteristic of temperature independent linear dielectric response with the variation in frequency (ω) is frequently observed in low loss materials.[25] Even otherwise it is confirmed that the low loss materials show flat dielectric response rather than loss peaks. These experimental observations point to the fact that charge carrier-frame work ion interactions remain unaffected in magnitude with temperature and frequency so that the values of n remain constant.

Figures 5(a) and 5(b) show the ln σ_{dc} and the ln ω_h for the as-quenched glass plotted as functions of inverse temperature $(1000/T)$. Increase in the σ_{dc} and the ω_h with temperature is due to the increase in the thermally activated mobility of ions according to hopping conduction mechanism. The plots are linear and the processes therefore are thermally activated through Arrhenius equations

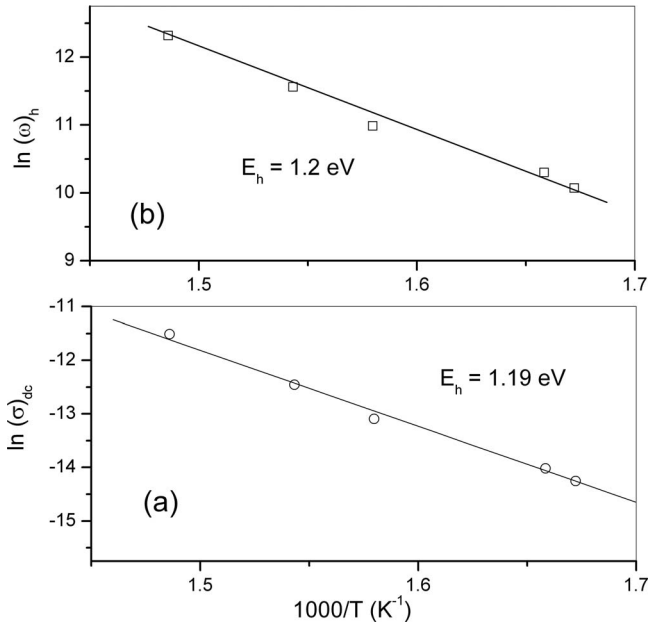

FIG. 5. Arrhenius plots of (a) dc conductivity and (b) hopping frequency for the as-quenched SBBO glass.

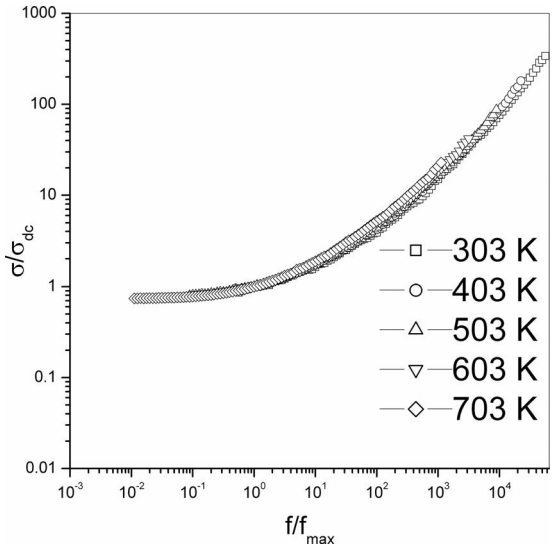

FIG. 6. Master plot of the normalized σ_{dc} conductivity vs normalized frequency.

$$\sigma_{dc} = \sigma_0 \exp\left(-\frac{E_{dc}}{kT}\right), \tag{2}$$

$$\omega_H = \omega_0 \exp\left(-\frac{E_h}{kT}\right), \tag{3}$$

where σ_0 and E_{dc} are the dc conductivity pre-exponential factor and conductivity activation energies for mobile ions, ω_0 and E_h, are the pre-exponential factor and the activation energy for hopping frequency, respectively. The activation energies E_h and E_{dc} are almost identical. This indicates that at reasonably high temperatures, charge transport is governed by a single energy barrier, and no additional mechanism become operative in the dc conduction (flat σ region). Reduced Almond–West type power law fit is shown in Fig. 6, which represents the master plot of ac conductivity for the as-quenched SBBO glass. The required frequency ω_o has been obtained from plots of imaginary part of the electrical modulus (see latter), and the conductivity has been scaled by the dc conductivity σ_{dc}. The curves superimpose very well, implying that a single mechanism of ion transport is in operation over the range of temperatures under study.

B. Complex impedance spectroscopy analysis

The resistive and capacitive components of the impedance of the glass can be estimated by impedance spectroscopy. Figure 7 shows the impedance (Z' versus Z'') plots for the as-quenched SBBO at four different temperatures (573, 598, 623, and 648 K). These Cole–Cole plots[29] display semicircles with depressed centers. This behavior is typical of systems in which a distribution of relaxation times is present. The electrical response can also be investigated using electrical modulus formalism. Modulus is derived from the impedance data by equation $M^*(\omega) = j\omega C_0 Z^*(\omega)$, where $j = \sqrt{-1}$

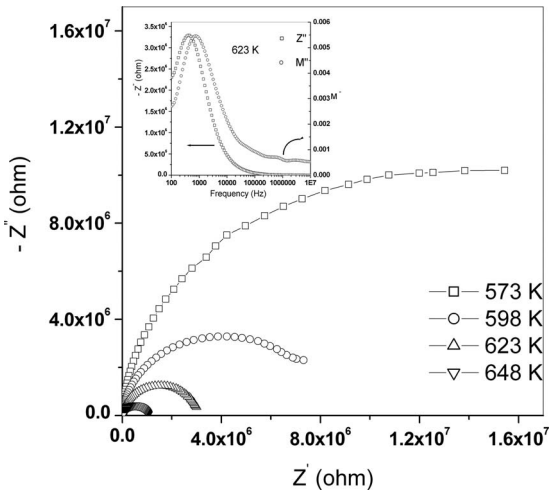

FIG. 7. Complex impedance plots at four different temperatures for the as-quenched SBBO glass; inset shows the imaginary part (Z'') of impedance and (M'') modulus as a function of frequency at 623 K.

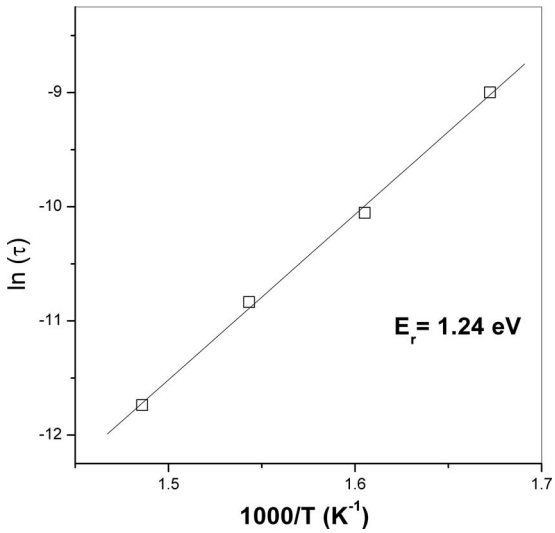

FIG. 9. Arrhenius plot of relaxation times (τ) for the as-quenched SBBO glass.

and C_0 is the vacuum capacitance of the cell. In the modulus representation the effect of electrode polarization contributions gets suppressed, which is sometimes helpful in elucidating mechanism of relaxation. Additionally the modulus analysis often provides a better understanding of polarization phenomena than the analysis of impedance alone. The inset of Fig. 7 shows the Z'' and M'' as functions of frequencies at 623 K. The Z'' (ω) exhibits a peak at slightly lower frequency than M'' (ω) and also decreases at high frequencies faster. It implies that the electrode surface makes a small non-negligible contribution to the measured dielectric parameters at high frequencies. Further Z'' (ω) frequency plot appears as if the asymmetric M'' (ω) peak is shifted toward the lower frequencies. The slight mismatch of the peaks and asymmetry development may be attributed to the non-Debye relaxation behavior. In order to rationalize the impedance data, an equivalent circuit composed of a resistance R and capacitance C in parallel (as shown in the inset of Fig. 8) was analyzed. The parallel RC element results in a semicircle in an impedance plot. The Z' versus Z'' plots where the x-axis and the impedance curve cross over at low frequency is the bulk resistance R. The equivalent circuit can be expressed by the Cole–Cole function[30,31]

$$Z^* = \frac{R}{[1 + (j\omega\tau)^{\alpha}]}, \tag{4}$$

where $\tau = RC$ and α characterizes a weight on the distribution of the relaxation times with the values ranging from 0 to 1. For an ideal Debye relaxation $\alpha = 1$ and the full width at half maximum (FWHM) of Z'' peak is 1.14 decades. $0 < \alpha < 1$ implies that the process is governed by a distribution of relaxation times, which leads to a broader than Debye relaxation peak. Separating the real and imaginary parts of Eq. (4), we can write

$$Z' = \frac{R\left\{1 + (\omega\tau)^{\alpha}\sin\left[(1-\alpha)\frac{\pi}{2}\right]\right\}}{1 + (\omega\tau)^{2\alpha}\sin\left[(1-\alpha)\frac{\pi}{2}\right]}, \tag{5}$$

$$Z'' = \frac{R(\omega\tau)^{\alpha}\cos\left[(1-\alpha)\frac{\pi}{2}\right]}{1 + (\omega\tau)^{2\alpha}\sin\left[(1-\alpha)\frac{\pi}{2}\right]}. \tag{6}$$

Fitting the experimental data to the above expression for Z'' [Eq. (6)] is shown in Fig. 8. It is evident from Fig. 8 that the experimental curves are remarkably well fitted using Eq. (6) in the entire range of frequencies and temperatures under study.

Figure 9 shows the dependence of the relaxation time on the reciprocal temperatures. It clearly suggests that the relaxation time follows the Arrhenius equation

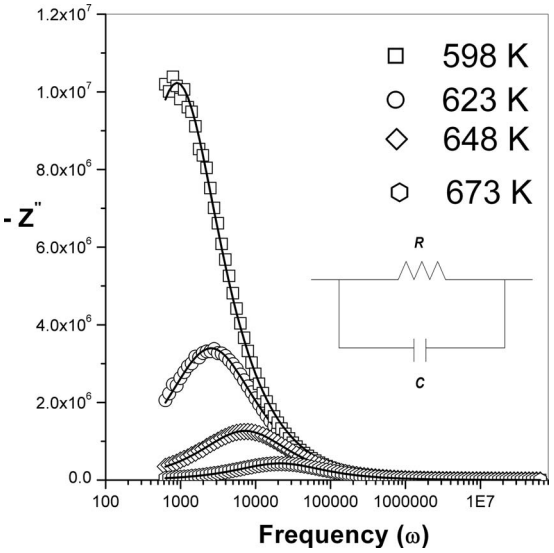

FIG. 8. The frequency dependence of Z'' at four various temperatures; the solid lines indicate the theoretical fit.

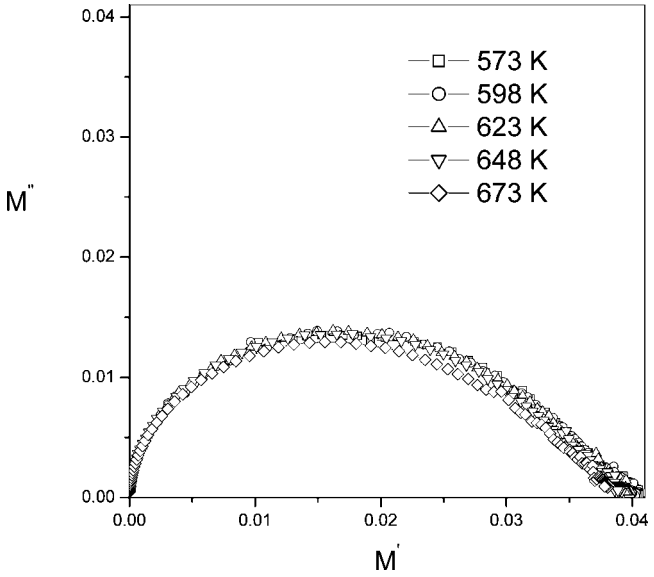

FIG. 10. Plot of M' and M'' at various frequencies.

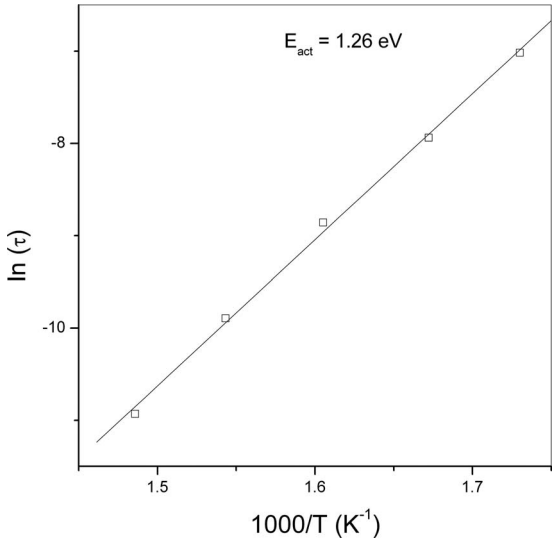

FIG. 12. Arrhenius plot of relaxation times (τ) for the as-quenched SBBO glass.

$$\tau = \tau_o \exp\left(\frac{E_r}{k_B T}\right), \tag{7}$$

where τ_o is the prefactor and E_τ is the activation energy for the relaxation. E_τ is found to be 1.24 eV from the slope.

Figure 10 shows the complex modulus plots of the as-quenched SBBO glass at different temperatures. There appears to be prominent (single) semicircle consistent with the single phase character of the as-quenched SBBO. The frequency dependence of real part of modulus (M') at various temperatures is shown in Fig. 11(a). M' reaches a maximum value $M_\infty = 1/\varepsilon_\infty$ at higher frequencies and tends toward zero at low frequencies, which suggest significant electrode polarization.[32]

Figure 11(b) shows the frequency variation of $M''(\omega)$ at different temperatures. $M''(\omega)$ exhibits a peak and the position of the peak shifts toward higher frequencies with increasing temperature. The peaks are all asymmetric and centered in the corresponding dispersion region of M'. The charge carriers may be considered as mobile over long distances at frequencies lying to the left of the peaks. In the region to the right of the peak, charge carrier ion motion is generally confined and the immediate neighborhood of the potential well. This region of the peak therefore is indicative of the transition from long range dominated to short range dominated mobility.[33] The frequency $f_{\max}$ (corresponding to $M''_{\max}$) gives the most probable conduction relaxation time (τ_σ) from the condition $2\pi f_{\max} = 1$. Its variation as a function of temperature is shown in Fig. 12. This plot also obeys the Arrhenius relation

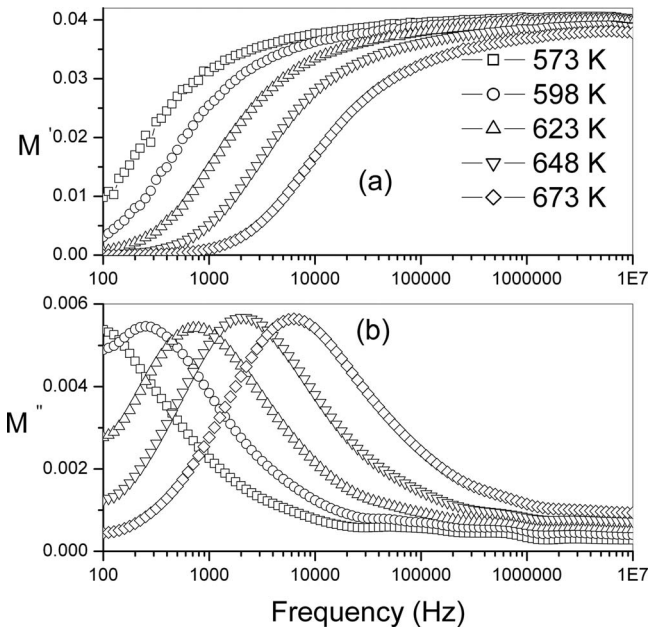

FIG. 11. Frequency dependence of the (a) real (M') and (b) imaginary (M'') part of electric modulus for the as-quenched SBBO glass.

$$\tau_\sigma = \tau_{\sigma o} \exp\left(\frac{E_a}{k_B T}\right), \tag{8}$$

where $\tau_{\sigma 0}$ is the pre-exponential factor and E_a is the activation energy. The activation energy E_a calculated from the linear fit to the data points is again 1.26 eV, which is consistent with the activation energies from the temperature dependence of hopping frequencies from the dc conductivity measurements.

Modulus-frequency master plot is shown in Fig. 13 for the SBBO glasses investigated in this work. The scaling behavior of the electrical modulus is quite evident. There is near perfect overlap of data over the whole range of temperatures with almost constant FWHM of the reduced frequency peak. However, FWHM is greater than the width of a typical Debye peak (1.14 decades). Thus it appears that the charge dynamics from long range to short range in these phases is characterized by a constant activation energy, which is also independent of both temperature and frequency. The master plot [Fig. 13(b)] can also be analyzed in terms of a stretched exponential decay function with a stretching exponent β,[34]

$$\phi(t) = \exp(-t/\tau_0)^\beta, \quad 0 < \beta < 1, \tag{9}$$

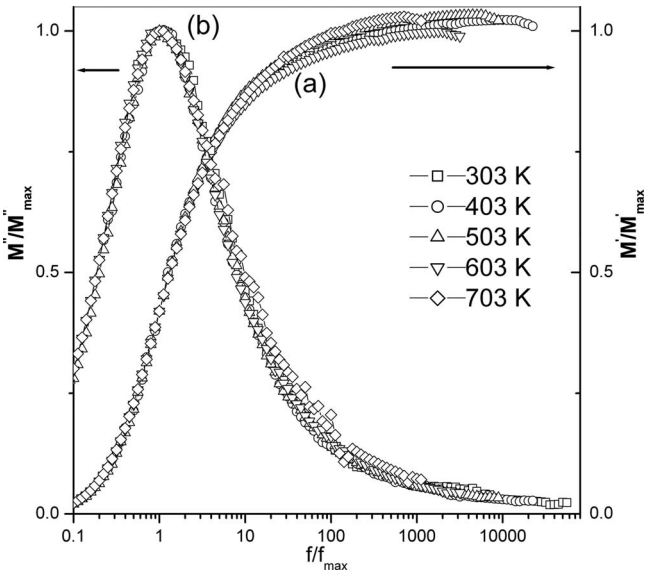

FIG. 13. Modulus master plots of (a) real and (b) imaginary parts of the modulus for the as-quenched SBBO at different temperatures.

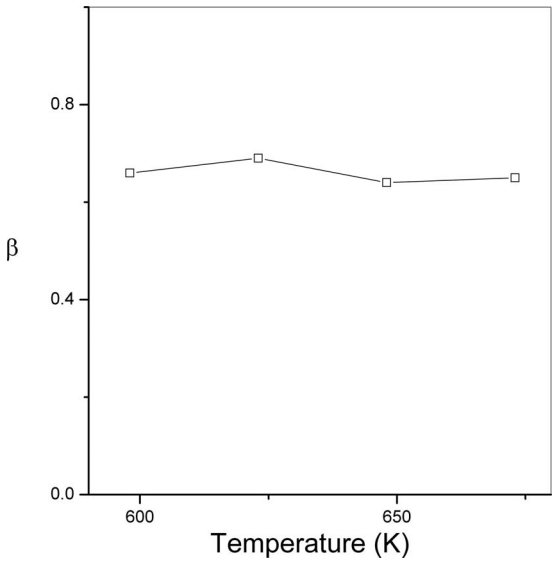

FIG. 14. Variation in β with temperature.

where τ_o is the characteristic relaxation time and $\varphi(t)$ represents the time decay of an electric field. Parameter β is a measure of slowing down of the relaxation time. $\beta=1$ corresponds to the ideal Debye solid with a unique relaxation time. $\beta=0$ corresponds to maximum interaction of dipoles with other dipoles.[33] The function $\varphi(t)$ is related to the modulus in the frequency domain by the equation

$$M^* = M' + jM'' = M_\infty \left\{ 1 - \int_0^\infty dt \exp(-i\omega t)[-d\phi(t)/dt] \right\}, \quad (10)$$

where M_∞ is the limiting high frequency real part of the modulus. From the master plots it is clearly seen that FWHM values are invariant with temperature, suggesting that the parameter β has a constant value. The value of β can be obtained by fitting the spectrum at each temperature by the method of Moynihan.[35] Figure 14 shows the temperature dependence of β. The values of β are nearly constant, lie between 0.5 and 0.6, and are also insensitive to the variation in temperature. Since a distribution of relaxation times would render β sensitive to temperature, it appears that stretched exponential nature of relaxation is the likely origin of the non-Debye behavior in these glasses. We also note that in passing in the present glass system, the power law exponent (n) and stretching exponent (β) are not related as $n+\beta=1$.[36–38]

In summary our observations point to the following. (i) The charge transport occurs through an activated process. (ii) The activation behavior obtained from different (although in principle related) methods are nearly equal (1.25 eV) in value. (iii) The dielectric behavior confirms that the loss peaks occur with characteristic stretched exponential behavior. (iv) However, the exponent from simple West–Almond conductivity-frequency relation is found to be not related to the stretching exponent β from dielectric moduli-frequency behavior. (v) Both n and β however are found to be essentially temperature independent. Therefore we would like to see if a common transport mechanism explains our observations.

In the first place we note that the measured activation barrier of 1.25 eV is significantly lower than expected because oxygen is not present as a free O^{-2} ion and in order to create O^{-2} ion, either a $Bi-O^-$ or a $B-O^-$ bond has to be broken. This is in addition to the motional barrier. It is also unlikely that the activation barrier corresponds to migration of the divalent Sr^{+2} cation. We also do not suspect transport by a combination of Sr^{+2} and O^{-2}. We suggest that the charge transport in SBBO glasses occur via direct participation of nonbridging oxygens (NBOs), which carry a single negative charge. We propose that NBOs switch their positions on the three dimensionally connected bismuth borate network. Both B and Bi are well known to be capable of having three and four coordination in glasses.[39–41] A tetrahedral B can exchange a NBO with either a trigonal B or a three coordinated Bi, leading to effective transport of NBO and hence a charge. To make it more clear we designate trigonal $[BO_{3/2}]^o$ and tetrahedral B $[BO_{4/2}]^-$ as B_3 and B_4 and three coordinated $[BiO_{3/2}]^o$ and pyramidal $[BiO_{4/2}]^-$ as Bi_3 and Bi_4, respectively. The charge transport is visualized to take place as

$$[B_3]^o + [B_4]^- \rightarrow [B_4]^- + [B_3]^o \;\; ; \;\; B_3^o + [B_4]^- \rightarrow [B_4]^- + [B_3]^o,$$

$$[Bi_3]^o + [Bi_4]^- \rightarrow [Bi_4]^- + [Bi_3]^o \;\; ; \;\; [B_3]^o + [B_4]^- \rightarrow [Bi_4]^- + [B_3]^o.$$

All that is required is a less energetic local structural rearrangement. The structural rearrangement on bismuth borate network can be expected to be quite facile. The activation barrier can be significantly lower because the charged oxygen atom in NBO is not physically displaced. In the activated state, only the coordination around network forming B/Bi atoms changes as visualized below.

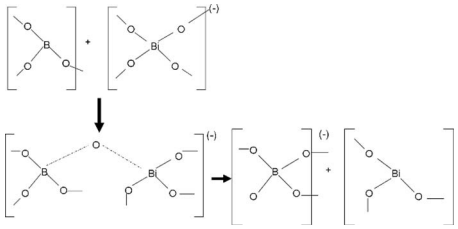

It has been shown elsewhere[42–45] that such a mechanism can also account for the existence of stretched exponential behavior. Briefly the reason is as follows. When the NBO switches from one position to the other via an activated state, only one stage of relaxation will be over. That is because the cation, which was in nearest neighborhood of NBO prior to switching, gets marginally destabilized by virtue of the increased distance from NBO. Therefore it drifts to the neighborhood of the NBO, and only after that the final state becomes energetically almost identical with its earlier value in the new structural position.

Therefore there are two components to the total relaxation: the first from the activated state to the switched over position and the second from switched over state to final state. The second relaxation process starts after a times delay. If $\varphi_1(t)$ and $\varphi_2(t)$ are the two relaxation processes with characteristic relaxation times τ_1 and τ_2,

$$\varphi_1(t) = \varphi_1(o)e^{t/\tau_1}, \quad \varphi_2(t) = \varphi_2(o)e^{(t-t_o)/\tau_2}.$$

It is assumed that both relaxations are Debye type. The observed overall relaxation $\varphi(t)$ will be the sum of $\varphi_1(t)$ and $\varphi_2(t)$. Such a sum behaves effectively as

$$\varphi(t) = \phi_1(t) + \phi_2(t) = \varphi_1(o)e^{t/\tau_1} + \varphi_2(o)e^{(t-t_o)/\tau_2} \approx \psi_1(o)\exp\left[\frac{t}{\tau}\right]^{\beta}.$$

Such functional equivalence has been shown to hold good earlier[42–45]

Thus observed single β appears to be quite reasonable. That a single barrier observed is due to the fact that the process of NBO jump is the primary energetic step. The rearrangement step involving drift of Sr^{+2} ion may not be a "jump" process in the usual sense and is sort of a drift of the position of Sr^{+2} toward a lower energy state. Perhaps the observation of a single temperature independent β can be associated with the dominant first activation barrier in the above expression. The second cation drifting step may occur with a much lower activation barrier for τ_2.

IV. CONCLUSIONS

$SrBi_2B_2O_7$ glasses have been investigated using a number of experimental techniques. Ion transport has been studied over a range of frequencies and temperatures. The observed properties have been examined in the light of existing models in the literature. Structural modification has also been examined. Structural rearrangement on borate-bismuthate network is considered as facile. ac conductivities exhibit simple power law variation. Both ac conductivities and moduli have been found to be collapsible on to master plots, suggesting the presence of a common charge transport mechanism in these glasses. A model that considers transport as due to the NBO switching has been proposed in which a two stage relaxation appears natural. This structural model consistently accounts for all the observations made in the present investigation. The relaxation process is most likely through stretched exponential behavior.

[1] W. Dumbaugh, Phys. Chem. Glasses **19**, 121 (1978).
[2] S. Simon and M. Todea, J. Non-Cryst. Solids **352**, 2947 (2006).
[3] B. Venkataraman and K. B. R. Varma, Opt. Mater. (Amsterdam, Neth.) **28**, 1423 (2006).
[4] F. Borsa, D. Torgeson, S. Martin, and H. Patel, Phys. Rev. B **46**, 795 (1992).
[5] Y. Dimitriev, V. Mihailova, and E. Gattef, Phys. Chem. Glasses **34**, 114 (1986).
[6] W. Mianxue and Z. Peinan, J. Non-Cryst. Solids **84**, 344 (1986).
[7] Y. Cheng, H. Xiao, and W. Guo, Thermochim. Acta **444**, 173 (2006).
[8] H. Zheng and J. Mackenzie, Phys. Rev. B **38**, 7166 (1988).
[9] H. Zheng, R. Xu, and J. Mackenzie, J. Mater. Res. **4**, 911 (1989).
[10] D. Hall, M. Newhouse, N. Borrelli, W. Dumbaughand, and D. Weidman, Appl. Phys. Lett. **54**, 1293 (1989).
[11] M. Onishi, M. Kyoto, and M. Watanabe, Jpn. J. Appl. Phys., Part 2 **30**, L988 (1991).
[12] M. G. El-Shaarawy and F. H. El-Batal, Phys. Chem. Glasses **43**, 247 (2002).
[13] Y. B. Saddeek, E. R. Shaaban, EI. S. Moustafa, and H. M. Moustafa, Physica B **403**, 2399 (2008).
[14] E. R. Shaaban, M. Shapaan, and Y. B. Saddeek, J. Phys.: Condens. Matter **20**, 155108 (2008).
[15] P. Becker, Adv. Mater. (Weinheim, Ger.) **10**, 979 (1998).
[16] N. S. Prasad and K. B. R. Varma, J. Mater. Chem. **11**, 1912 (2001).
[17] G. S. Murugan and K. B. R. Varma, J. Mater. Chem. **12**, 1426 (2002).
[18] G. S. Murugan and K. B. R. Varma, Mater. Res. Bull. **34**, 2201 (1999).
[19] Y. Takahashi, Y. Benino, T. Fujiwara, and T. Komatsu, J. Appl. Phys. **89**, 5282 (2001).
[20] Q. Zhao, X. Zhu, X. Bai, H. Fan, and Y. Xie, Eur. J. Inorg. Chem. **2007**, 1829 (2007).
[21] R. Ihara, T. Honma, Y. Fujiwara, and T. Komatsu, Opt. Mater. (Amsterdam, Neth.) **27**, 403 (2004).
[22] J. Barbier, N. Penin, A. Denoyer, and L. M. D. Cranswick, Solid State Sci. **7**, 1055 (2005).
[23] J. Barbier and L. M. D. Cranswick, J. Solid State Chem. **179**, 3958 (2006).
[24] K. Majhi and K. B. R. Varma, J. Non-Cryst. Solids **354**, 4543 (2008).
[25] A. K. Jonscher, *Dielectric Relaxation in Solids* (Chelsea Dielectric, London, 1983).
[26] D. P. Almond and A. R. West, Nature (London) **306**, 456 (1983).
[27] E. F. Hairetdionv, N. F. Uvarov, H. K. Patel, and S. W. Martin, Phys. Rev. B **50**, 13259 (1994).
[28] L. C. Costa and F. Henry, Phys. Chem. Glasses **44**, 353 (2003).
[29] K. S. Cole and R. H. Cole, J. Chem. Phys. **9**, 341 (1941).
[30] J. S. Kim, H. S. Lee, and C. H. Jeong, J. Korean Phys. Soc. **42**, 1042 (2003).
[31] J. E. Kim, S. J. Kim, J. H. Cho, and Y. S. Yang, J. Korean Phys. Soc. **35**, 1449 (1999).
[32] B. V. R. Chowdari and R. Gopalkrishnan, Solid State Ionics **23**, 225 (1987).
[33] H. K. Patel and S. W. Martin, Phys. Rev. B **45**, 10292 (1992).
[34] C. T. Moynihan, L. P. Boesch, and N. L. Laberge, Phys. Chem. Glasses **14**, 122 (1973).
[35] C. T. Moynihan, J. Non-Cryst. Solids **172–174**, 1395 (1994).
[36] A. Pan and A. Ghosh, Phys. Rev. B **59**, 899 (1999).
[37] J. E. Kim, S. J. Kim, and Y. S. Yang, Mater. Sci. Eng., A **487**, 304 (2001).

[38]K. L. Ngai, J. Non-Cryst. Solid **203**, 232 (1996).
[39]Z. Lin, Z. Wang, C. Chen, and M. H. Lee, J. Appl. Phys. **90**, 5585 (2001).
[40]V. C. Veeranna Gowda, C. Narayana Reddy, K. C. Radha, R. V. Anavekar, J. Etourneau, and K. J. Rao, J. Non-Cryst. Solids **353**, 1150 (2007).
[41]M. Bosca, L. Pop, G. Borodi, P. Pascuta, and E. Culea, J. Alloys Comp. **479**, 579 (2009).
[42]M. H. Bhat, M. Ganguli, and K. J. Rao, Curr. Sci. **86**, 676 (2004).
[43]S. Kumar, P. Vinatier, A. Levasseur, and K. J. Rao, J. Solid State Chem. **177**, 1723 (2004).
[44]M. H. Bhat, M. Kandavel, M. Ganguli, and K. J. Rao, Bull. Mater. Sci. **27**, 189 (2004).
[45]S. Kumar and K. J. Rao, Solid State Ionics **170**, 191 (2004).